Mass renormalization in the bandwidth-controlled Mott-Hubbard systems $SrVO_3$ and $CaVO_3$ studied by angle-resolved photoemission spectroscopy

T. Yoshida,[1] M. Hashimoto,[1] T. Takizawa,[1] A. Fujimori,[1] M. Kubota,[2] K. Ono,[2] and H. Eisaki[3]
[1]*Department of Physics, University of Tokyo, Bunkyo-ku, Tokyo 113-0033, Japan*
[2]*Photon Factory, KEK, Tsukuba, Ibaraki 305-0801, Japan*
[3]*National Institute of Advanced Industrial Science and Technology, Tsukuba 305-8568, Japan*
(Received 26 February 2010; published 30 August 2010)

$Ca_{1-x}Sr_xVO_3$ is a Mott-Hubbard-type correlated electron system whose bandwidth can be varied by the V-O-V bond angle but the actual effect of bandwidth control on the electronic structure has been controversial in previous photoemission experiments. In this work, band dispersions and Fermi surfaces of $SrVO_3$ and $CaVO_3$ are studied by angle-resolved photoemission spectroscopy. Near the Fermi level (E_F), three bands forming cylindrical Fermi surfaces derived from the three V $3d$ t_{2g} orbitals have been observed. The observed bandwidths for both compounds are almost half of those predicted by local-density approximation band-structure calculation, confirming mass renormalization caused by electron correlation. It has been clearly demonstrated that the width of the d band in $CaVO_3$ is narrower than that in $SrVO_3$, qualitatively consistent with the result of band-structure calculation. Roles of the orthorhombic lattice distortion and electron correlation in the observed band narrowing are discussed.

DOI: 10.1103/PhysRevB.82.085119 PACS number(s): 71.18.+y, 71.20.−b, 71.27.+a, 71.30.+h

The complex nature of correlated electrons in transition-metal oxides (TMOs) causes various interesting phenomena including high-T_c superconductivity and colossal magnetoresistance.[1] Light transition-metal oxides such as perovskite-type Ti and V oxides are ideal systems to study the fundamental physics of electron correlation because they are prototypical Mott-Hubbard-type systems, in which the O $2p$ band is located below the transition-metal $3d$ band, in the framework of the Zaanen-Sawatzky-Allen classification scheme.[2] Those systems have a relatively small number of electrons in the degenerate t_{2g} bands, and their electronic properties have been modeled by the Hubbard model without explicit consideration of the oxygen p orbitals. In the Mott-Hubbard regime, the MIT occurs when the ratio of the on-site Coulomb repulsion (U) to the one-electron bandwidth (W) exceeds a critical value $(U/W)_c$. In those light TMOs, the electronic properties are those of normal Fermi liquids on the metallic side while they are Mott insulators (with orbital ordering) on the insulating side of the metal-insulator transition (MIT). Electron correlation effects and MITs in light TMOs have been described based on theoretical predictions of dynamical mean-field theory (DMFT) for the Hubbard model.[3]

To address the nature of electron correlation in light TMOs experimentally, photoemission spectroscopy has provided rich information. In the photoemission spectra of the perovskite-type Ti and V oxides,[4–7] the coherent part around the Fermi level (E_F) corresponding to bandlike electronic excitations and incoherent part 1–2 eV away from E_F corresponding to atomiclike excitations or the remnant of the lower Hubbard band have been observed. DMFT has predicted that the effective mass of conduction electron is enhanced concomitant with decreasing spectral weight in the coherent part[3] and that spectral weight transfer occurs from the coherent part to incoherent part as the system approaches an MIT from the metallic side. For example, in the filling-controlled Mott-Hubbard system $La_{1-x}Sr_xTiO_3$, a critical mass enhancement occurs toward the MIT according to the electronic specific heats γ and the magnetic susceptibility χ.[8] The doping dependence of photoemission spectral weight and of the bandwidth of the coherent part indeed reflects the behaviors of γ and χ as predicted by DMFT.[7] On the other hand, the effective-mass enhancement and spectral weight transfer in the bandwidth-controlled Mott-Hubbard system $Ca_{1-x}Sr_xVO_3$ (CSVO) have been controversial. In CSVO, the V-O-V angle varies with x and the bandwidth decreases with decreasing x. Early photoemission results have shown that, with decreasing x, i.e., with decreasing bandwidth, spectral weight is transferred from the coherent part to the incoherent part[4] in a dramatic way compared to the moderate enhancement of γ.[9] In contrast, according to a bulk-sensitive photoemission study using soft x rays, neither appreciable spectral weight transfer nor appreciable band narrowing has been observed for $SrVO_3$ and $CaVO_3$.[10] On the other hand, another bulk-sensitive photoemission study using a laser has revealed the suppression of spectral weight near E_F in going from $SrVO_3$ to $CaVO_3$.[11] Thus, the difference in the electronic structure between $SrVO_3$ and $CaVO_3$ still remains unclear. To reconcile the discrepancies between the different experiments caused by overlapping surface and bulk signals, angle-resolved photoemission spectroscopy (ARPES) turned out to be a powerful method, as demonstrated by the successful ARPES observation of band dispersions and Fermi surfaces in $SrVO_3$.[12] In that study, mass renormalization which is consistent with γ and reflects the bulk electronic properties could be identified. The result has been confirmed by a subsequent ARPES study using epitaxially grown thin films of $SrVO_3$ with high surface quality.[13] The agreement between the thin-film and the single-crystal results indicates that the energy dispersions of the quasiparticle bands are not significantly affected by the surface conditions. However, how the electronic structure changes with bandwidth control in CSVO has not been studied using ARPES. In order to address this issue, in the present work, we have performed an

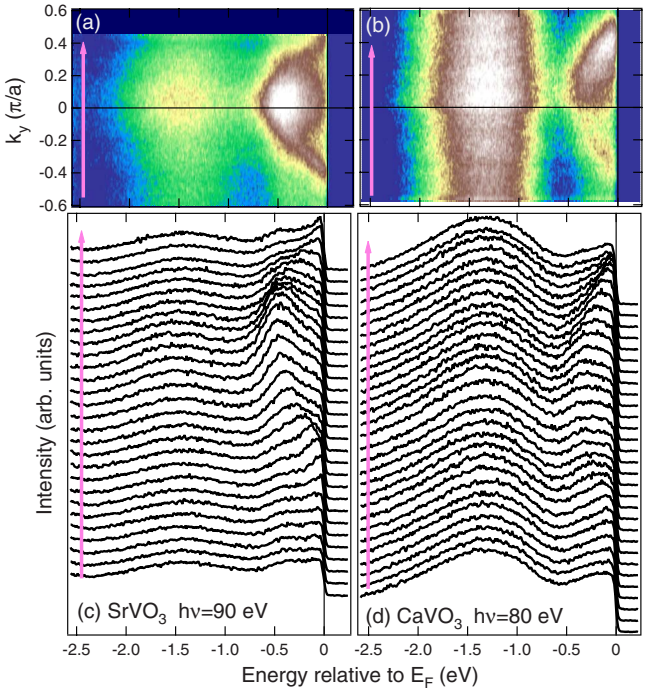

FIG. 1. (Color online) ARPES spectra of $SrVO_3$ and $CaVO_3$ along the k_y direction with k_x=0 in the first Brillouin zone. [(a) and (b)] Intensity plot of $SrVO_3$ and $CaVO_3$ in the E-k_y plane. [(c) and (d)] Corresponding EDCs. The dispersive feature within ~0.7 eV of E_F is the coherent part while the broad feature centered around 1.3–1.5 eV below E_F is the incoherent part.

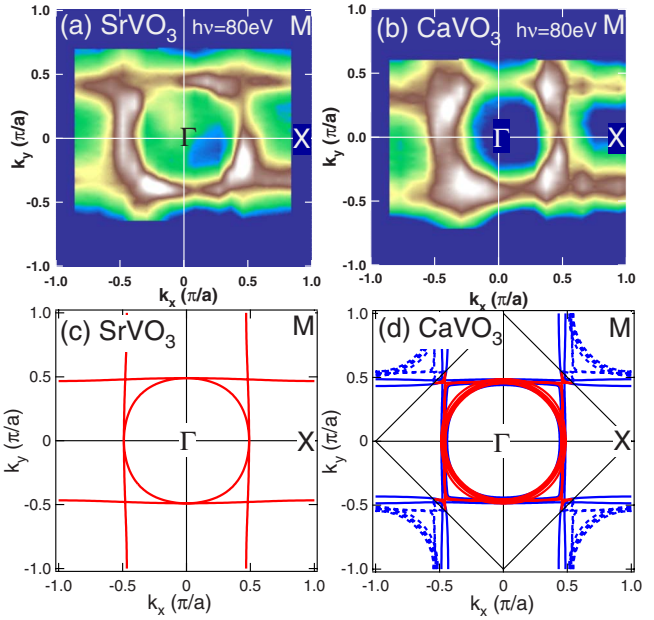

FIG. 2. (Color online) Spectral weight mapping at E_F for (a) $SrVO_3$ and (b) $CaVO_3$ using $h\nu$=80 eV. Spectral weight has been integrated within 20 meV of E_F. Note that the mapping is a projection on the k_x-k_y plane. [(c) and (d)] Fermi-surface cross sections by the k_z=0 plane (red curves) predicted by band-structure calculation (Ref. 15). For $CaVO_3$, Fermi-surface cross sections by the k_y=0 and k_x=0 planes and folded Fermi surfaces due to the orthorhombic distortion are indicated by overlapping blue solid and dashed curves, respectively.

ARPES study of $SrVO_3$ and $CaVO_3$. In going from $SrVO_3$ to $CaVO_3$, one would expect that the observed band dispersions reflect band narrowing effects both due to orthorhombic lattice distortion and electron correlation. In this work, we have clearly observed the narrower bandwidth in $CaVO_3$ than that in $SrVO_3$, which is quantitatively consistent with the specific-heat coefficient γ. By comparing the ARPES results with the results of band-structure calculations,[14,15] the effects of the orthorhombic lattice distortion and electron correlation on the observed mass renormalization are discussed.

ARPES measurements were performed at beamline 28A of Photon Factory with a Scienta SES-2002 electron analyzer. The typical energy and angular resolutions were about 30 meV and 0.3°, respectively. Single crystals of $SrVO_3$ and $CaVO_3$ were grown by the traveling-solvent floating zone method. Samples were first aligned *ex situ* using Laue diffraction, cleaved *in situ* along the cubic (100) surface at 20 K and measured at the same temperature in a pressure better than 1×10^{-10} Torr. We used circularly polarized photons with energies from $h\nu$=47 to 100 eV. In this paper, the electron momentum is expressed in units of π/a, where a=3.84 Å (3.76 Å) for $SrVO_3$ ($CaVO_3$) is the cubic lattice constant corresponding to the V-V distance. k_x and k_y are the momenta parallel to the cleavage plane and k_z is the momentum perpendicular to the plane.

First, we show energy distribution curves (EDCs) of $SrVO_3$ and $CaVO_3$ for k_x=0 with various k_y's in Fig. 1. The coherent part within ~0.7 eV of the Fermi level (E_F) shows a clear dispersive feature corresponding to the calculated band structure. The incoherent part, which reflects electron correlation, centered at ~−1.5 eV and ~−1.3 eV for $SrVO_3$ and $CaVO_3$, respectively, shows appreciable momentum-dependent intensities as seen in Figs. 1(a) and 1(b). The intensity is stronger within the Fermi surface ($k_y<k_F$), consistent with the previous ARPES study on thin films and the results of DMFT calculation.[13]

Spectral weight at E_F in the first Brillouin zone is mapped in k_x-k_y space for $SrVO_3$ and $CaVO_3$ in Figs. 2(a) and 2(b), respectively, for photon energy $h\nu$=80 eV. Fermi surfaces for $SrVO_3$ and $CaVO_3$ predicted by band-structure calculation[15] are shown in Figs. 2(c) and 2(d), respectively. For $SrVO_3$, the overall feature of the mapped Fermi surface is in good agreement with the band-structure calculation. The observed spectral weight distribution indicates the cylindrical Fermi surfaces consisting of the three t_{2g} orbitals, the d_{xy}, d_{yz}, and d_{zx} orbitals, of vanadium. Particularly, we have observed a cross section or a projection of the cylindrical Fermi surface derived from the d_{yz} orbital and that from the d_{zx} orbital. These Fermi surfaces are extended along the k_x and k_y directions and were not clearly observed in the previous study.[12] The result of the spectral weight mapping for $CaVO_3$ is similar to that of $SrVO_3$ but the momentum distribution is generally broader than $SrVO_3$ because the crystal structure of $CaVO_3$ is orthorhombic and band folding occurs due to the quadrupling of the unit cell as shown in Fig. 2(d). Since the cleaved surface may contain *ab*, *bc*, and *ac* planes, the observed ARPES spectra would be a superposition of the dispersions from the *ab*, *bc*, and *ac* surfaces. Such folded bands

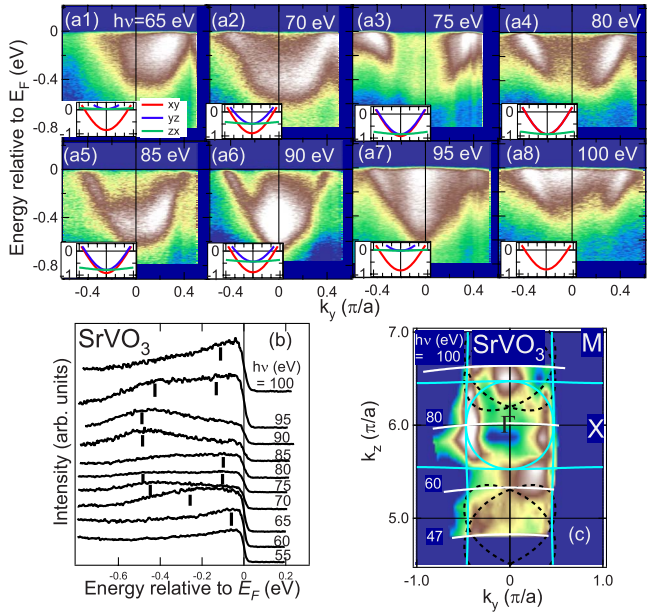

FIG. 3. (Color online) ARPES spectra of $SrVO_3$ in the E-k_y plane for various photon energies corresponding to various k_z's. (a1)–(a8): photon-energy dependence of the ARPES spectra near the normal emission. Insets are band dispersions for corresponding cuts predicted by band-structure calculation (Ref. 15). (b) Normal emission spectra. (c) Intensity at E_F mapped in the k_y-k_z plane. Fermi surfaces predicted by band-structure calculation (Ref. 15) are shown by blue curves. Black dotted curves indicate the d_{yz} Fermi surfaces from secondary cones.

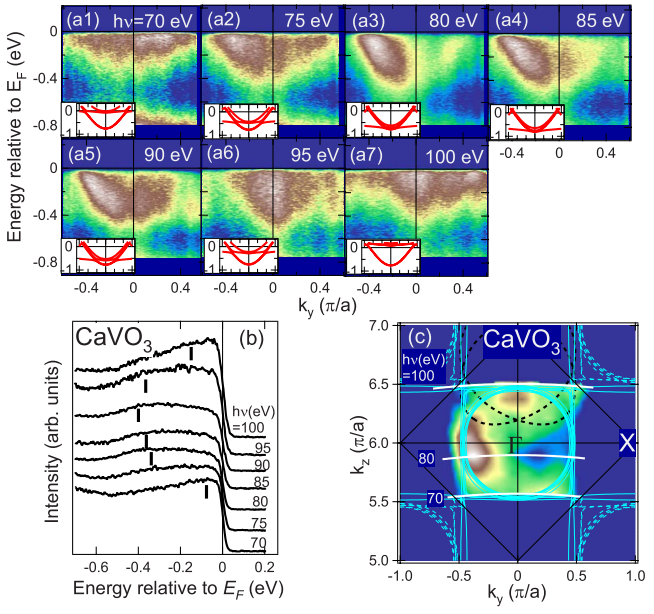

FIG. 4. (Color online) ARPES spectra of $CaVO_3$ for various photon energies corresponding to various k_z's. (a1)–(a7): photon-energy dependence of the ARPES spectra around the normal emission. Insets are band dispersions for corresponding cuts predicted by band-structure calculation (Ref. 15). (b) Normal emission spectra. (c) Intensity at E_F mapped in k_y-k_z space. Fermi surfaces predicted by band-structure calculation (Ref. 15) are shown by blue curves. Black dotted lines indicate d_{yz} Fermi surfaces from secondary cones.

of different orientations are not resolved in the present spectra and would give rise to the broad spectral weight distribution compared to that in $SrVO_3$.

Figures 3(a) and 4(a) show the photon-energy dependence of the ARPES spectra of $SrVO_3$ and $CaVO_3$, respectively, for k_x=0 cuts along the k_y direction. The asymmetry of the ARPES intensity with respect to k_y=0 is due to matrix-element effects of the circular polarized light. The observed parabolic band is the d_{xy} band, which has nearly two-dimensional electronic structure in the k_x-k_y plane parallel to the sample surface. Spectral features of $CaVO_3$ are broader than those of $SrVO_3$, which may be due to the orthorhombic crystal distortion of $CaVO_3$. For $SrVO_3$, we have observed enhanced spectral weight at −0.4 eV for $h\nu \sim 90$ eV and this enhanced part moves toward the Fermi level with increasing photon energy. This enhancement is due to the overlap of the bottom $d_{yz,zx}$ band because the matrix element of the d_{xy} orbital is suppressed around $k_x=k_y=0$. Therefore, the shift of the intensity with photon energy indicates the energy dispersion of the $d_{yz,zx}$ bands along the k_z direction. This behavior is also predicted by the band calculation[15] as shown in the insets. In the case of $CaVO_3$, the intensity of the $d_{yz,zx}$ bands are not so strong as in $SrVO_3$. Nevertheless, the flat dispersions near E_F corresponding to the $d_{yz,zx}$ bands are observed around $h\nu$=70 and 100 eV, indicating the Fermi surface crossing of these bands along the k_z direction. Figures 3(b) and 4(b) are normal-emission spectra for various photon energies. We have also mapped ARPES intensities at E_F in the k_y-k_z plane in order to reveal the cross section of the d_{yz} FS, as shown in Figs. 3(c) and 4(c). Here, the k_z values have been obtained from $h\nu$'s assuming the inner potential of V_0=17 eV. These mapping patterns for both samples qualitatively agree with the Fermi surfaces obtained from the band-structure calculation as demonstrated in Figs. 3(c) and 4(c). Note that, in the previous ARPES study, signals from the $d_{yz,zx}$ bands were unclear, probably due to surface effects,[12] while we have clearly observed these bands in the present results. We should also remark that there are structures with weak intensity which are not predicted by the band calculation as shown in Fig. 3(c). This may represent photoelectrons from secondary cones.[16] Assuming that the emitted electrons receive the in-plane reciprocal vector $\mathbf{G}=(\pm 2\pi, \pm 2\pi)$, we have simulated the d_{yz} Fermi surface from secondary cones and explained the observed intensity distribution, as indicated by dashed curves in Figs. 3(c) and 4(c). In addition to these extrinsic features, we also consider a possible existence of surface states. In our previous ARPES study,[12] we have discussed several possible origins of surface states such as surface reconstruction and the discontinuity of the potential at the surface. In the present study, these surface structures have not been identified. Thus, we concluded that the present results also reflect bulk electronic structure.

In order to investigate electron correlation effects for both samples, we have determined the quasi-particle (QP) dispersion near Γ point ($h\nu \sim 80$ eV for $SrVO_3$ and $h\nu \sim 85$ eV for $CaVO_3$). Figures 5(a) and 5(b) show the same ARPES spectra as Fig. 3 (a4) and Fig. 4 (a4), respectively, with QP

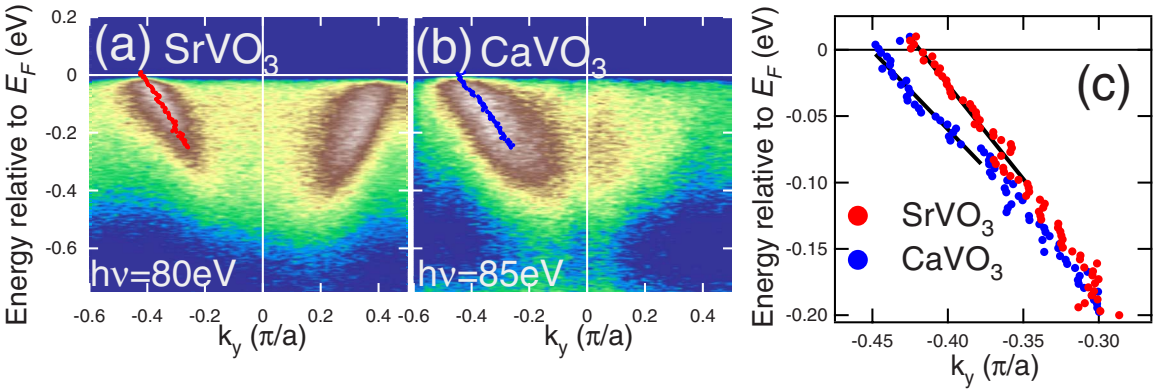

FIG. 5. (Color online) Comparison of band dispersions in $SrVO_3$ and $CaVO_3$. ARPES spectra of (a) $SrVO_3$ and (b) $CaVO_3$ along the Γ-X lines. The observed band is the d_{xy} band. (c) Quasiparticle dispersions determined by the MDC peak positions.

dispersions determined by the peak positions of momentum distribution curves (MDCs). The QP dispersions for both compounds are compared in Fig. 5(c). From the slope of the dispersions within ~0.1 eV from the E_F, we have deduced the Fermi velocity $v_F \sim 1.7$ eV Å and ~1.4 eV Å for $SrVO_3$ and $CaVO_3$, respectively. This corresponds to the observation that the binding energy of the bottom of the d_{yz} band for $CaVO_3$ is ~0.4 eV [Fig. 4(b)] while it is ~0.5 eV for $SrVO_3$ [Fig. 3(b)]. Assuming the two-dimensional cylindrical Fermi surfaces for the three t_{2g} orbitals, the electronic specific-heat coefficient γ has been estimated from the observed v_F to be $\gamma \sim 7.5$ mJ mol^{-1} K^{-2} and ~9.0 mJ mol^{-1} K^{-2} for $SrVO_3$ and $CaVO_3$, respectively, which are close to the experimental values of 8.18 ($SrVO_3$) and 9.25 ($CaVO_3$) mJ mol^{-1} K^{-2}.[9] Therefore, the observed mass renormalization in the QP dispersions are quantitatively consistent with the electronic specific-heat coefficient γ within the Fermi-liquid picture. From these results, it is experimentally confirmed that $CaVO_3$ has a narrower QP bandwidth than $SrVO_3$ while this has been unclear in the previous photoemission studies.[4,10,11] Now, let us discuss possible mechanisms of the band narrowing in these materials. The observed bandwidths for both $SrVO_3$ to $CaVO_3$ are nearly half of those predicted by the band-structure calculation. This can be attributed to electron correlation as local-density approximation (LDA)+DMFT calculations explain the mass renormalization by a factor of ~2 if a moderate Coulomb interaction U is assumed.[17]

In going from $SrVO_3$ to $CaVO_3$, the additional band narrowing has been observed as described above. The observed Fermi velocity indicates an increase in the effective mass m^* up to 18%. This band narrowing may be interpreted in terms of either the orthorhombic lattice distortion or electron correlation or both of them. In the simple tight-binding description of the band structure of the perovskite-type oxides, the effective hopping parameter between neighboring d orbitals is proportional to $\cos^2\theta$, where θ is the V-O-V bond angle. In $SrVO_3$ and $CaVO_3$, $\cos^2\theta$ is ~1 ($\theta \sim 180°$) and $\cos^2\theta \sim 0.88$ ($\theta \sim 160°$), respectively, yielding a band narrowing by ~12%. The LDA calculation by Pavarini *et al.*[15] has predicted the narrowing by ~16%. However, another LDA calculation by Nekrasov *et al.*[14] indicates band narrowing only by ~4%, and this small narrowing is explained by the increasing hopping parameter between nearest-neighbor d orbitals in $CaVO_3$. If we employ the LDA calculation by Nekrasov *et al.*,[14] i.e., if we assume that the LDA band mass m_b increases by ~4%, the present results indicate that m^*/m_b increases by ~10% in going from $SrVO_3$ to $CaVO_3$, consistent with the scenario that U/W increases and hence enhances m^*/m_b through electron correlation in going from $SrVO_3$ to $CaVO_3$. However, the DMFT calculation[14] based on their LDA band structures does not exhibit the appreciable band narrowing from $SrVO_3$ to $CaVO_3$. Therefore, the effect of the increasing d-d hopping in $CaVO_3$ could not be identified in our experimental result. If we employ the LDA calculation by Pavarini *et al.*, on the other hand, the present results indicate that the electron mass enhancement factors m^*/m_b for both compounds are nearly the same between $SrVO_3$ and $CaVO_3$ and therefore that there are no appreciable difference in electron correlation strengths in both compounds. If this interpretation is correct, U/W should not increase appreciably in going from $SrVO_3$ to $CaVO_3$. One possible scenario for the nearly constant U/W is that the on-site Coulomb interaction U is reduced by hybridization between the V 3d orbitals and the d orbitals of the A-site cation in going from $SrVO_3$ to $CaVO_3$. If the orthorhombic distortion in $CaVO_3$ enhances the hybridization between these orbitals, the net density of 3d electrons at the V site may decrease, resulting in the reduction in U. In fact, the binding energy of the incoherent peak, which is approximately $\sim U/2$ according to the DMFT results, decreases from ~1.5 eV in $SrVO_3$ to ~1.3 eV in $CaVO_3$ as shown in Fig. 1.

Although clear band narrowing from $SrVO_3$ to $CaVO_3$ has been observed in the quasiparticle dispersions, the angle-integrated spectra taken by soft x ray show almost no difference between them. The discrepancy may stem from differences in the linewidths of the quasiparticles. As seen in the present data, the linewidths of the spectra of $CaVO_3$ are larger than those of $SrVO_3$. Thus, the effect of the broadening on the angle-integrated spectra would be larger in $CaVO_3$, resulting in nearly no difference between the spectra for both samples.

In conclusion, we have studied the energy dispersions and the Fermi surfaces of the three-dimensional Mott-Hubbard systems $SrVO_3$ and $CaVO_3$ by ARPES. The observed bandwidths for both samples are almost half of those predicted by the band-structure calculation, consistent with the DMFT calculation[17] where the mass renormalization is caused by electron correlation. We have confirmed that the width of the V $3d$ band indeed decreases by $\sim 20\%$ in going from $SrVO_3$ to $CaVO_3$. The observed mass renormalization in the d band near E_F can explain the moderate mass enhancement in γ from $SrVO_3$ to $CaVO_3$. This band narrowing can be explained by the orthorhombic distortion and possibly by additional increase in correlation strength caused by the increase in U/W.

We are grateful to M. Rozenberg for enlightening discussions and N. Kamakura for technical support. This work was supported by a Grant-in-Aid for Scientific Research (S) (Grant No. 22224005) and a Grant-in-Aid for Young Scientists (B) (Grant No. 22740221) from the Japan Society for the Promotion of Science (JSPS). This work was done under the approval of the Photon Factory Program Advisory Committee (Proposal No. 2006S2-001).

[1] M. Imada, A. Fujimori, and Y. Tokura, Rev. Mod. Phys. **70**, 1039 (1998).
[2] J. Zaanen, G. A. Sawatzky, and J. W. Allen, Phys. Rev. Lett. **55**, 418 (1985).
[3] A. Georges, G. Kotliar, W. Krauth, and M. J. Rozenberg, Rev. Mod. Phys. **68**, 13 (1996).
[4] I. H. Inoue, I. Hase, Y. Aiura, A. Fujimori, Y. Haruyama, T. Maruyama, and Y. Nishihara, Phys. Rev. Lett. **74**, 2539 (1995).
[5] K. Morikawa, T. Mizokawa, K. Kobayashi, A. Fujimori, H. Eisaki, S. Uchida, F. Iga, and Y. Nishihara, Phys. Rev. B **52**, 13711 (1995).
[6] A. Fujimori, I. Hase, H. Namatame, Y. Fujishima, Y. Tokura, H. Eisaki, S. Uchida, K. Takegahara, and F. M. F. de Groot, Phys. Rev. Lett. **69**, 1796 (1992).
[7] T. Yoshida, A. Ino, T. Mizokawa, A. Fujimori, Y. Taguchi, T. Katsufuji, and Y. Tokura, Europhys. Lett. **59**, 258 (2002).
[8] K. Kumagai, T. Suzuki, Y. Taguchi, Y. Okada, Y. Fujishima, and Y. Tokura, Phys. Rev. B **48**, 7636 (1993).
[9] I. H. Inoue, O. Goto, H. Makino, N. E. Hussey, and M. Ishikawa, Phys. Rev. B **58**, 4372 (1998).
[10] A. Sekiyama, H. Fujiwara, S. Imada, S. Suga, H. Eisaki, S. I. Uchida, K. Takegahara, H. Harima, Y. Saitoh, I. A. Nekrasov, G. Keller, D. E. Kondakov, A. V. Kozhevnikov, Th. Pruschke, K. Held, D. Vollhardt, and V. I. Anisimov, Phys. Rev. Lett. **93**, 156402 (2004).
[11] R. Eguchi, T. Kiss, S. Tsuda, T. Shimojima, T. Mizokami, T. Yokoya, A. Chainani, S. Shin, I. H. Inoue, T. Togashi, S. Watanabe, C. Q. Zhang, C. T. Chen, M. Arita, K. Shimada, H. Namatame, and M. Taniguchi, Phys. Rev. Lett. **96**, 076402 (2006).
[12] T. Yoshida, K. Tanaka, H. Yagi, A. Ino, H. Eisaki, A. Fujimori, and Z. X. Shen, Phys. Rev. Lett. **95**, 146404 (2005).
[13] M. Takizawa, M. Minohara, H. Kumigashira, D. Toyota, M. Oshima, H. Wadati, T. Yoshida, A. Fujimori, M. Lippmaa, M. Kawasaki, H. Koinuma, G. Sordi, and M. Rozenberg, Phys. Rev. B **80**, 235104 (2009).
[14] I. A. Nekrasov, G. Keller, D. E. Kondakov, A. V. Kozhevnikov, T. Pruschke, K. Held, D. Vollhardt, and V. I. Anisimov, Phys. Rev. B **72**, 155106 (2005).
[15] E. Pavarini, A. Yamasaki, J. Nuss, and O. K. Andersen, New J. Phys. **7**, 188 (2005).
[16] G. Mahan, Phys. Rev. B **2**, 4334 (1970).
[17] E. Pavarini, S. Biermann, A. Poteryaev, A. I. Lichtenstein, A. Georges, and O. K. Andersen, Phys. Rev. Lett. **92**, 176403 (2004).